Available online at www.sciencedirect.com
SCIENCE DIRECT®

Journal of the European Ceramic Society 23 (2003) 9–18

www.elsevier.com/locate/jeurceramsoc

High temperature sintering of SiC with oxide additives: II. Vaporization processes in powder beds and gas-phase analysis by mass spectrometry

S. Baud[a], F. Thévenot[a], C. Chatillon[b,*]

[a]*Ecole Nationale Supérieure des Mines de Saint-Etienne, 158 cours Fauriel, 42023 Saint-Etienne Cedex 2, France*
[b]*Laboratoire de Thermodynamique et Physico-Chimie Métallurgiques (INPG/UJF/CNRS UMR 5614), ENSEEG, BP 75 38402 St Martin d'Hères, France*

Received 20 August 2001; received in revised form 25 February 2002; accepted 11 March 2002

Abstract

The liquid phase sintering process of SiC using Al_2O_3–Y_2O_3 oxide mixture is performed in a temperature range where some matter loss occurs by vaporization. When using a buffer bed of SiC + Al_2O_3 powder mixture, this matter loss cannot be entirely counteracted and some transfer of matter—alumina—is observed between the green pellets and the beds. The present mass spectrometric study is aimed to the identification of the gaseous species that vaporize from such a bed placed in Knudsen cells in the 1350-1750 K temperature range. The Al(g), Al_2O(g), SiO(g) and CO(g) species are identified and their relative pressures measured as a function of alumina composition, crucible materials and excess of C or Si. Differences show that some non-equilibrium vaporization processes occur. In addition, the vaporization of impurities as well as C, Si or SiO_2 excess leads to a rapid decrease of their content and influence during the heating first stage before sintering.

Keywords: Mass spectrometry; SiC (Al_2O_3–Y_2O_3); Sintering; Vaporisation

1. Introduction

SiC sintering is usually performed at very high temperature ~2200 °C with some B_4C-C additives. In order to decrease this sintering temperature, a liquid phase has been tentatively used, the main components of this liquid being Al_2O_3 and Y_2O_3, the composition of the liquid being close to the eutectic in the range YAG–Al_2O_3. In this case, the sintering temperature could be decreased to the 1800–2000 °C range, but the ceramists observed large weight losses[1–6] of the SiC and/or additives compounds. In order to decrease these weight losses, a buffer bed of SiC + Al_2O_3 large grains powders is used, either arranged as alternate layers or as mixed powders, that surround the green compacts of SiC + additives to be sintered. The whole system is then usually placed in a graphite vessel, more or less completely closed by a cover in which small holes are drilled for initial pumping before filling with Argon.

Owing to the high temperature operation of this sintering process, the weight losses are attributed to vaporization of the mixtures SiC + Al_2O_3 used as buffer beds accompanied by matter exchanges between the bed and the compacts. Rather simple qualitative explanations of these losses have tentatively been made based on arbitrarily choosen elementary chemical reactions,[1,7,8] but their conclusions are necessarily inaccurate because they do not take into account some of the processes that occur in the quaternary Al–C–O–Si-system, as revealed by complete thermochemical analysis of the behavior of the SiC–Al_2O_3 pseudobinary system[9,10] in the whole Al–C–O–Si quaternary. The congruent vaporization behavior of the SiC–Al_2O_3 pseudobinary section has been demonstrated[10] and explains clearly the loss of matter observed after sintering experiments, but some experimental confirmation is needed.

The present mass spectrometric study is aimed (i) at the characterization of vaporization processes occurring for the SiC–Al_2O_3 mixed powders in their practical environmental conditions—graphite and alumina crucibles—including the behavior of impurities (this, part II),

* Corresponding author.
E-mail address: chatillo@ltpcm.inpg.fr (C. Chatillon).

0955-2219/02/$ - see front matter
PII: S0955-2219(02)00068-7

(ii) at the evaluation of partial vapor pressures and related kinetic processes that lead to "hindered" or "retarded" vaporization of the powder beds (part III) and (iii) at the exchange of species by vapors between the bed and the samples (part IV).

2. Experimental

The Knudsen-cell mass spectrometry is a method used since 1954 that has increased greatly the capability of analysis of vapors at high temperature.[11–14] Indeed, data compiled and treated in thermochemical tables[15–18] for the pure compounds SiC and Al_2O_3 and used for our previous thermochemical analysis (part I) of this SiC–Al_2O_3 pseudobinary system[10] are obtained mainly by this experimental technique—at least for gaseous molecules that vaporize from these compounds. We use this technique in order to compare the real behavior of our powder beds with the predicted one from our previous thermochemical analysis.[10]

2.1. The Knudsen effusion method

Samples are placed in a closed vessel—a Knudsen cell[19]—the lid of which has been drilled with a small orifice (Fig. 1). For material chemical compability reasons and in order to be able to use different crucible and lid materials—dense and pure graphite or alumina—our cells are built as a crucible and lid assembly, surrounded by a tantalum envelope in order to facilitate thermal equilibrium in the whole cell assembly. The pertinent parameter in the effusion technique is the ratio of gas effused through the orifice to the gas flow coming back to the vaporizing surface, that is the ratio $f = sC/S$. S is taken as the cross-section of the inner cell (crucible), s the cross-section and C the Clausing[19,20] coefficient or transmission probability of the orifice. When vaporization and condensation reactions are quite rapid it is generally assumed that a ratio $f \cong 10^{-2}$ is sufficient to reach equilibrium partial pressures in the cells.

The effusion cells are working under vacuum, and good evacuation conditions have to be assumed in order to prevent any reverse effused flow from the vacuum housing into the cells and this condition becomes important when non condensible gases—as CO in our case—effuse. For this reason our furnaces and their housings are built and fitted with large pumping capacities.[21]

Temperature measurements are performed either by a 6/30 PtRh thermocouple (Fig. 1) or by pyrometry [monochromatic, Leeds and Norpthrop, calibrated at NBS (1969)]. The secondary standards silver and gold melting points, as measured in our cells, or calibrations against the thermocouple are used in order to check the window absorption and to perform related corrections. A standard deviation ± 5.3 K is obtained in these calibration procedures and we can evaluate the temperature uncertainty to be $\delta T = \pm 10$ K.

In order to intercompare directly either the same samples or different powder mixtures, we also used the multiple cell method:[22–24] four cells are placed in a single isothermal block (Fig. 2). This method will be more extensively used in part III when analyzing the response from different orifice sizes in order to characterize quantitatively the vaporization kinetics.

The sample materials are those used for buffer beds in the sintering of SiC: SiC (Carborundum, with mean diameter grains $d = 99$ μm) or SiC (SIKA NOR IV, F120, from Norton, with $d = 109$ μm) and Al_2O_3 (BACO LS3, ALCAN, mean diameter 6.5 μm). For some experiments performed in triphasic domains Si +

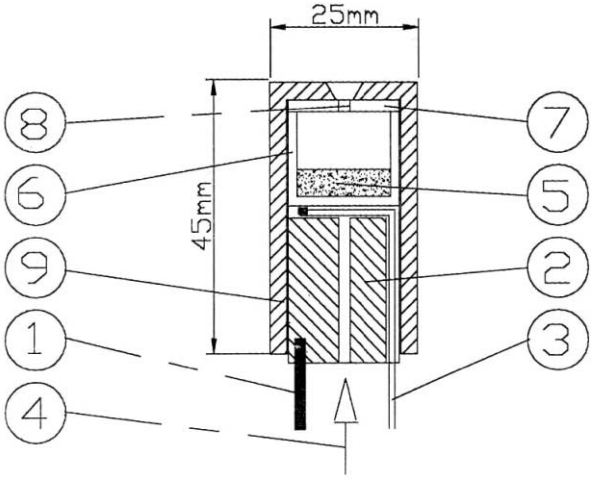

Fig. 1. Single conventional Knudsen effusion cell. 1: Three tungsten poles. 2: Tantalum holder. 3: Thermocouple. 4: Pyrometric sighting. 5: Sample (powder bed). 6: Crucible (dense Al_2O_3 or dense graphite). 7: Lid in the same material as the crucible. 8: Effusion orifice. 9: Tantalum envelope.

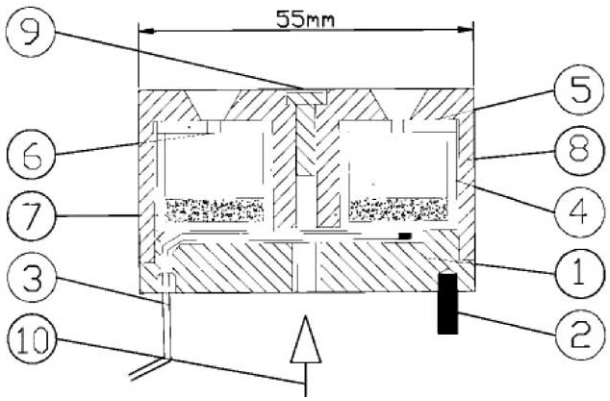

Fig. 2. Multiple effusion cell with four effusion cells. 1: Tantalum holder. 2: Three tungsten poles. 3: Thermocouple. 4: Crucible. 5: Lid. 6: Effusion orifice. 7: Samples. 8: Tantalum envelope. 9: Tantalum cap, which closes the access to remove the multiple cell out of the furnace. 10: Pyrometric sighting.

SiC + Al_2O_3 and C + SiC + Al_2O_3, Si (99.9% from Prolabo) and graphite (Carbone Lorraine, 2114) powders were used.

2.2. The mass spectrometric Knudsen cell coupling

The center part, close to the normal to the orifice, of the effused molecular beam is collimated (Fig. 3) for introduction in the ionization chamber of the mass spectrometer. The ionization of molecules leads to single ions—at least for rather small ionization potentials—that are accelerated by an electric field through electrostatic lenses, then the ions are separated according to their mass/charge ratio (m/e) by a magnetic field (Nuclide Mass Spectrometer with radius 30.5 cm, 90°) and then collected on a secondary Electron Multiplier working in a pulse counting mode (yield = 1 whatever is the ion detected). The basic mass spectrometric relation is:[11–14]

$$p_i S_i = I_i T$$

where p_i and T are respectively the partial pressure of the i species, and the temperature in the Knudsen cell, and S_i and I_i the mass spectrometer sensitivity and the measured ionic intensity for the i species. The sensitivity S_i includes several factors,[25] some of these cannot be evaluated independently of a suitable calibration procedure for each kind of experiment. In our case, the sensitivity is written,

$$S_i = G\sigma_i f_i$$

G being a geometrical factor, σ_i the ionization cross-section of the parent molecule along the ionization channel used and f_i the isotopic abundance that is known exactly from combination of the original isotopic distribution of atoms. The usual sensitivity range is within 10^{-11} bar to 10^{-4} bar in the cell, the lower limit being related to the mass spectrometric performances, meanwhile the higher one corresponds to the upper limit of the free molecular flow conditions at the effusion orifice.

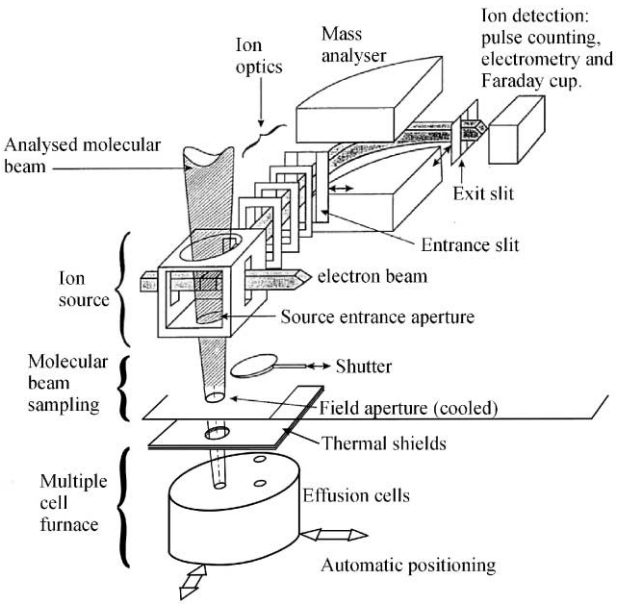

Fig. 3. Principle of the Knudsen-cell mass spectrometric coupling.

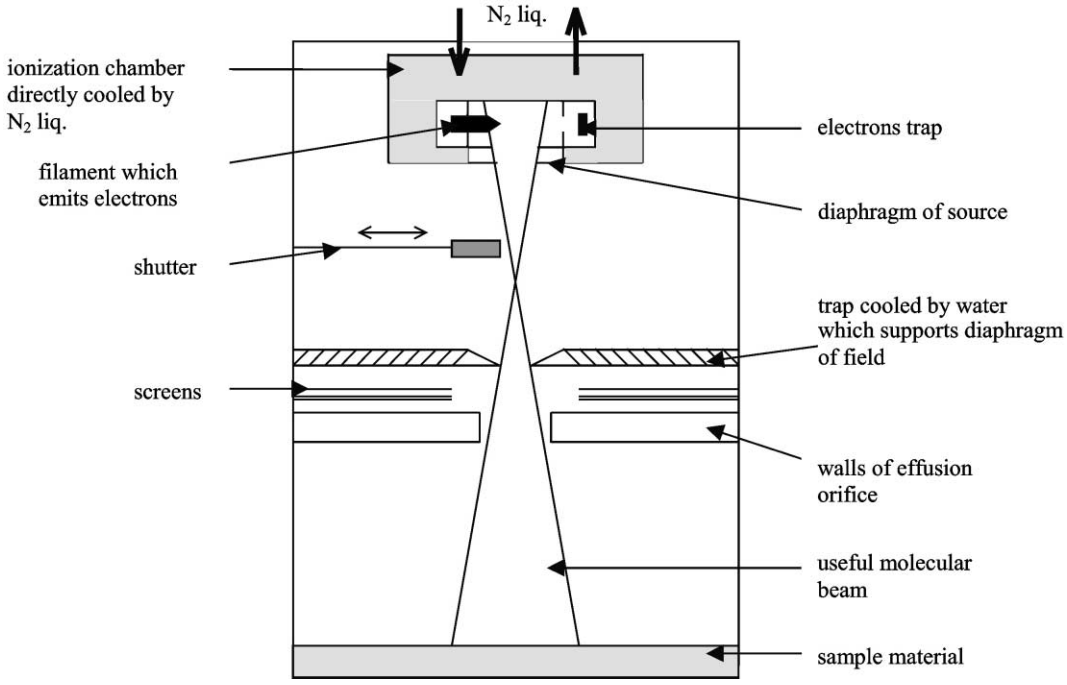

Fig. 4. Principle of our restricted collimation device used to sample the effused beam without any parasitic contributions.

In order to improve the mass spectrometric accuracy, we use a restricted collimation device[21] (Fig. 4) which is a prerequisite in such measurements for two main reasons:

- Parasitic contributions of molecules coming from other phenomena as external surface re-vaporizations [13,14,21,26]have to be discarded, mainly when using the multiple cell method which is sensitive to a few percent differences in ionic intensities,
- The comparison of pressures in cells with different orifices can be done directly since the geometrical factor G is defined as a true constant by the unique restricted collimation device attached to the mass spectrometer whatever is the measured cell.[21]

A shutter (Fig. 3) is used to distinguish molecules coming directly from the effusion orifice from those reflected from on any part of the instrument. For molecules the ions of which are not clearly separated from background atmosphere (CO/N_2), as well as those which are the same (CO) as existing in the background, we need a shutter located in such a position that its movement cannot interfere with background steady-state in the housings.[21]

At the beginning of each experiment, the ionic intensities are recorded as a function of cell position in order to locate correctly the cells on the axis of the restricted collimation device.[21–23] Then the position (X, Y) is stored and can be recalled at any time.

In this paper (part II of a series), we analyze the gas phase molecular composition in terms of $I_i{}^+T$ products which are equivalent to partial pressures. Further, we use the comparative measurements of ionic intensities of the same gaseous species vaporizing from different samples, or cells materials placed in the multiple cell in order to determine the nature of the vaporization processes, which may or may not be at equilibrium.[27]

3. Gas phase analysis

Thermodynamic calculations already performed in order to analyze the behavior of the SiC–Al_2O_3 pseudobinary system[9,10] showed that the four main gaseous species Al, Al_2O, CO and SiO vaporize in the detection range of our instrument and we were able to work quantitatively with these species. At the same time, the impurities in the SiC original powder (Al, Mg, Ca, Fe, Ni, Cr, Mn and SiO_2) as well as in the Al_2O_3 powder (Na_2O, SiO_2, Fe_2O_3/FeO, and CaO) may also give some volatile species that can interfere with gaseous species of our pseudobinary system, namely at mass 43 (AlO), 54 (Al_2 or Fe) where peaks were observed. Species at mass 28, CO, N_2, C_2H_4 (vacuum background) and Si were analyzed using the isotopic abundance at mass 30, and for impurities Cr, Fe, Mn and Ni, we systematically monitored the masses 52 to 60, to avoid some confusion with the Si_2(g) molecule if existing in the spectrum above the detection threshold.

Ions detected in the spectrum may also come from dissociative ionization when the ionization potential used is more than 3 or 4 volts above the ionization potential of the parent molecules ($\cong$ 6–14 volts). As an example, AlO^+ at mass 43 may come from:

$$AlO(g) + e^- \rightarrow AlO^+ + 2e^- \quad \text{adiabatic ionization}$$

or

$$Al_2O(g) + e^- \rightarrow AlO^+ + Al(g) + 2e^-$$

dissociative ionization

As we worked with electrons accelerated at about 30 V, these two processes may exist concurrently. In principle, and according to our previous thermodynamic analysis,[10] the first process must lead to very small ionic intensities because the pressure of the parent AlO(g) molecule is very low: from the ionic intensity measured at mass 43 the pressures of AlO(g) would be more than 11 000 times (at 1500 K) the previous calculated ones.[10] There is yet no doubt about the thermodynamic data of AlO(g) since they have been calculated from an assessed compilation and the difference of ionic intensities we observe is far from the assigned uncertainty range. The comparison of the ratios AlO^+/Al_2O^+ (Fig. 5) is another way to ascertain the molecular origin of AlO^+. The quite stable value, whatever is the temperature (contrarily to equilibrium constants), observed in our experiments attests the AlO^+ ion is a fragment ion issued from the molecule Al_2O(g). The mean value of the ratio $AlO^+/Al_2O^+ = 9.04 \pm 2.19\ 10^{-3}$ (at 30 V) agrees with the one already observed, $1.2\ 10^{-2}$ (at 30 V).[28] The slight and systematic evolution with temperature we observe in Fig. 5

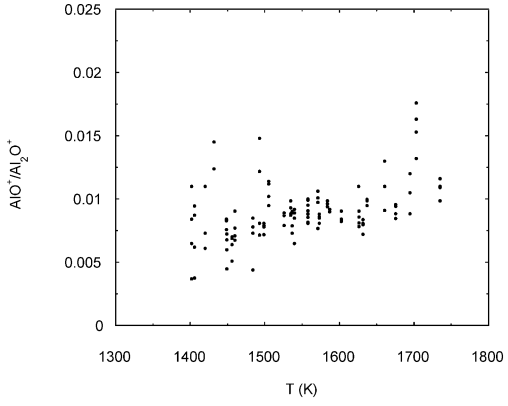

Fig. 5. Ionic intensity ratio AlO^+/Al_2O^+ as measured on the same cell at 30 V (ionizing voltage) as a function of temperature.

show some temperature influence on the relative yields of the two ionization channels. Our identification of the origin of AlO^+ ions rend earlier assumptions based on the evaporation of AlO(g) erroneous,[7] as well as raising some questions about the reliability of the AlO^+ measurements by quadrupole mass spectrometry.[29]

The peak at mass 54 was analyzed by isotopic abundance to be Al_2^+, discarding any Fe volatile impurity. The ratio Al_2^+/Al_2O^+ mean value is $4.29 \pm 1.6\ 10^{-3}$ (at 30 V) in quite good agreement with the earlier value $7.3\ 10^{-3}$,[28] or with indirect measured or calculated values respectively $5.5\ 10^{-3}$ and $2.26\ 10^{-3}$ [30] using the AlO^+/Al_2O^+ ratios as intermediate values. The peak Al_2^+ is thus effectively coming from the dissociative ionization of Al_2O(g) molecule. As the peak 54 may interfere with those of Cr and Fe isotopes, the further study of the impurities in SiC has been performed in the absence of alumina, with the advantage of a better sensitivity on the impurities due to the possibility of higher vaporization temperatures.

The analysis of the peak 28 after deduction of the CO contribution calculated from the peak at mass 30, reveals an apparent pressure of Si(g) 10 times higher than calculated by thermodynamics.[10] The ratio $Si^+/SiO^+ = 2.77 \pm 1.56\ 10^{-2}$ (at 30 V) is constant and lower than already observed (about 10–20%):[31] the Si^+ ion is thus a fragment ion from SiO(g), and no Si(g) was present in the gaseous phase. Conversely, the vaporization experiments of the triphasic SiC–Al_2O_3–C, show Si^+/SiO^+ ratios > 1: thus there exists another origin for the Si^+ ion since for this system the silicon activity and consequently the Si(g) vapor pressure decreases in the presence of an excess of carbon. We believe that some silicon carbonyls are formed in the gas phase. Indeed, the pressure of such species is very sensitive to the carbon activity and CO(g) pressure increases, when going from the Si–SiC–Al_2O_3 to the C–SiC–Al_2O_3 triphasic domain. We cannot corroborate our observations with thermodynamic calculations due to lack of literature data for these molecules.

As a conclusion, the gas phase analysis by mass spectrometry, confirms the presence of the main gaseous species as proposed by the thermodynamic analysis for the SiC–Al_2O_3 pseudobinary system:[9,10] Al, Al_2O, CO and SiO. These species are in quite similar proportion in the spectrum, and we are surprised that the mass spectrometric previous work[29] did not observe at least Al(g) and Al_2O(g) effusing with CO(g) and SiO(g). The presence in the spectrum of some fragment ions formed from these molecules that can interfere with impurities, led us to perform the impurity analysis only with pure compounds in order to obtain a better sensitivity threshold. In addition, indirect observations of a large contribution of Si^+ fragment ion led us to suppose that some silicon carbonyl gaseous species existed in the gas phase of the SiC–C–Al_2O_3 system.

4. Factors affecting the vapor pressures

Preliminary to determination of partial vapor pressures, the vaporization processes must be checked for: (i) impurities influence, (ii) ageing or non steady-state behavior.

The first item relates the behavior of the sintering process to the presence or not of impurities. If the initial impurity content is sufficient and the compositions remain quite constant through the sintering, some influence can be postulated. The second item deals with early stages of the sintering like for instance rapid reaction of smaller particles and their disappearance as well as evolution of the reactive surfaces. Further more, comparative measurements of partial vapor pressures using the multiple cell method, can reveal, with a high degree of accuracy and reliability, the attainment or not of equilibrium for vaporization experiments. At this stage, possibilities exist to further analyze the vaporization in terms of thermodynamics or kinetics.

4.1. Impurity vaporization

Alumina vaporization was studied with single cells (Fig. 1), firstly vaporizing the lone crucible and lid in Alumina, secondly loading the ALCAN Alumina powder. The main volatile impurity observed was Na, that distills rapidly at 1500 °C, followed by some traces of Mn. At that time the aluminum based species becomes largely predominant in the spectrum.

The two SiC powders—impurities Al, Fe, Mn, Ca, Ni and SiO_2—were vaporized in dense graphite cells. The two Al(g) and Fe(g) persistent species have similar vapor pressures for the two powders, although the Al(g) distillation seems more rapid from the carborundum powder. More important is the behavior of the SiO(g) species, which is a tracer of the initial SiO_2(s) content of the SiC, either as SiO_2 inclusions or more probably as thin coating layers. The evolution of the SiO(g) peak (the product IT being proportional to the pressure) is presented in Fig. 6 as a function of time along different temperature plateaus convenient for the mass spectrometric observation. The Norton SiC, the previous analysis of which reveals by X-ray measurements the presence of free silicon, produces higher SiO(g) vapor pressures, in agreement with thermodynamics of the Si–SiO_2–SiC system,[32,33] when compared with the Carborundum powder in which there is no free silicon. In addition, we have to quote that with Alumina in the beds, the oxygen potential will favor the loss of the SiO_2 coating layer due to the increase of the SiO(g) pressure, as opposed to any dissolution process of this layer into a liquid phase.

As a first conclusion, although the time scale of the mass spectrometric observation, as well as the ratio of the effused flow to the vaporizing one are not exactly the

same as those parameters used in the sintering processes, we can postulate that the sintering process will start with powders that have partly vaporised their impurities in the heating ramp, and probably lost the rest of them during the sintering. Moreover, the initial SiO_2(s) content would be lost quickly by SiO(g) vaporization even after the solubilisation in the liquid phase because the vaporization of SiC and oxides occurs with higher flows when the starting composition of the system does not correspond to the congruent pseudobinary section for which the vaporization flow is at a minimum as already discussed.[10]

4.2. Influence of SiC/Al_2O_3 molar ratios in the beds

According to thermodynamics, the composition in the $SiC–Al_2O_3$ pseudobinary section should not influence the partial pressures since no solubility range exists between the two compounds. However, as it was observed with $Si–SiO_2$ or SiO_2–SiC mixtures[31–33] in case of hindered vaporization, the number of contacts between the powder grains may influence the partial pressures. So, the multiple cell technique is used in order to compare different powder compositions (Table 1), as illustrated for Al(g) in Fig. 7. At the beginning of the experiment we always observe some evolutions of the pressure ratios (during about 4–4 h 30 min) before a relative stabilization. We retain a mean value for this stabilization stage (Table 1). We quote generally that the CO(g) pressure ratios are more scattered probably because the threshold for detection is dependent on the background and a correction is needed due to the Si^+ (fragment from SiO(g)) ion. Taking into account the quoted uncertainties, we can consider that the 5 and 15% Al_2O_3 mixtures vaporize identically since their partial pressures ratios are close to 1 (Table 1), meanwhile the equimolar mixture (71.8% weight), richer with alumina, produces higher SiO(g) pressures, lower pressures of CO(g), with the Al(g) and Al_2O(g) being less altered. These variations as a function of composition, contrarily to thermodynamics, prove that the vaporization is kinetically controlled. In addition, the increase of the SiO(g) pressure is necessarily related to contacts where this molecule is formed, i.e. $SiC–Al_2O_3$ contacts grains, since the mean free path of gases is larger than any distances in the cells (except for extreme high pressures $\cong 10^{-4}$ bar or high temperature stage). Thus similarity of partial pressures for the 5 and 15% alumina compositions may be related to the powders morphology (Fig. 8): the original 6.5 μm alumina is agglomerated into 100 μm balls and consequently the number of SiC (90 μm)–Al_2O_3 (100 μm) contacts between these two powders are not very different when compared to the number of contacts of the equimolar composition.

We observe generally that the SiO(g) pressure decreases with the alumina ratio, meanwhile the CO(g) pressure increases. Consequently the congruent ratio[10] Si flow/C flow = 1 cannot be maintained for at least one of these compositions, and the flow balance imposes that some samples are in the $SiC–C–Al_2O_3$ triphasic domains. Indeed the X-ray analysis of the 5 and 15% powders after experiments showed the presence of carbon conversely to the 71.8% which remains congruent ($SiC–Al_2O_3$). This behavior is not observed in the sintering process for the 7–15% ratios, probably because the temperature is in a higher range—2000–2200 K in place of 1550–1750 K in mass spectrometry. This difference in the behavior agrees with thermodynamic results[10] that pointed out a general evolution of the congruent behavior toward higher silicon activity and consequently lower C activities when the temperature increases.

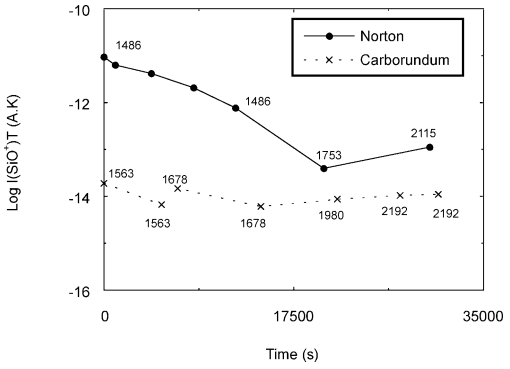

Fig. 6. Evolution of the decimal logarithm of the SiO(g) pressure (proportional to the I^+T products) with time along a typical experiment run with increasing temperature plateaus. Comparison of the two SiC powders.

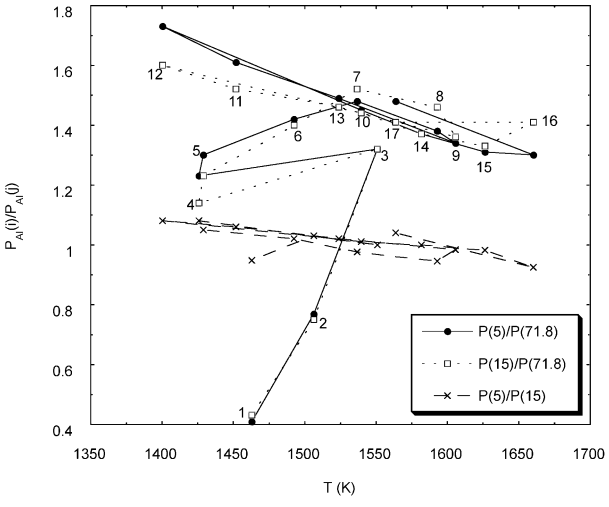

Fig. 7. Comparison of two aluminum pressures—from two cells in a multiple cell—loaded with different compositions (see Table 1) as a function of temperature. The numbers refer to successive different temperature plateaus along the experiment. *i* in *p*(*i*) refers to the Al_2O_3 composition in wt.% of the powder beds.

4.3. Influence of the crucible material

As the thermodynamic analysis[10] showed that SiC–Al_2O_3 is a congruent vaporization section, the choice of an alumina or SiC (coating graphite) crucible should not influence the vaporization process. In order to check this, we have chosen the same equimolar composition sample and compared the partial pressures between two cells, alumina and SiC coating on graphite (Table 2). Once again we observed some transient state before stabilization. The mean values of the partial pressure ratios show the same trend as with the preceding excess of alumina: SiO(g) pressure increased, meanwhile other species decreased. The analysis of the residues did not evidence any free carbon, and the decrease of SiO(g) in the graphite cell (coated with SiC) can be explained by the consumption of Si by the crucible according to the reaction,

$$2C(s) + SiO(g) \rightarrow CO(g) + SiC(s)$$

The SiC coating is attacked at its surface to create CO(g) in the gas phase, meanwhile the silicon moves inwards to restore the SiC coating at the SiC/C interface. The two reactions of vaporization/attack and diffusion/creation of SiC exist in a quasi steady-state flow with effusion. The existence of such a chain of reactions is confirmed during the sintering process when analyzing the deposit on the inner wall of graphite crucibles (Fig. 9): two layers were identified: graphite/Al_4SiC_4/SiC. The presence of Al_4SiC_4 confirms that Al participates in the diffusion process.

4.4. Influence of the SiC powder origin

As densification of samples during the sintering is dependent on the origin of SiC in the beds—carborundum or norton—we compared two beds SiC + Al_2O_3 formed with these two SiC and in the two crucibles, graphite and Al_2O_3 (Table 3). Once again the first five data (4 h 45 min including the initial mass spectrometric settings) showed a large evolution of ionic intensities. In the stable domain of measurements, all the measured partial pressures over the Norton SiC were lower by a factor of about 2 than those over the Carborundum SiC (Table 3). As the two SiC powders have similar granulometry, the pressure difference can come only from surface and related bulk physical properties as already observed for two different SiC powders.[34,35]

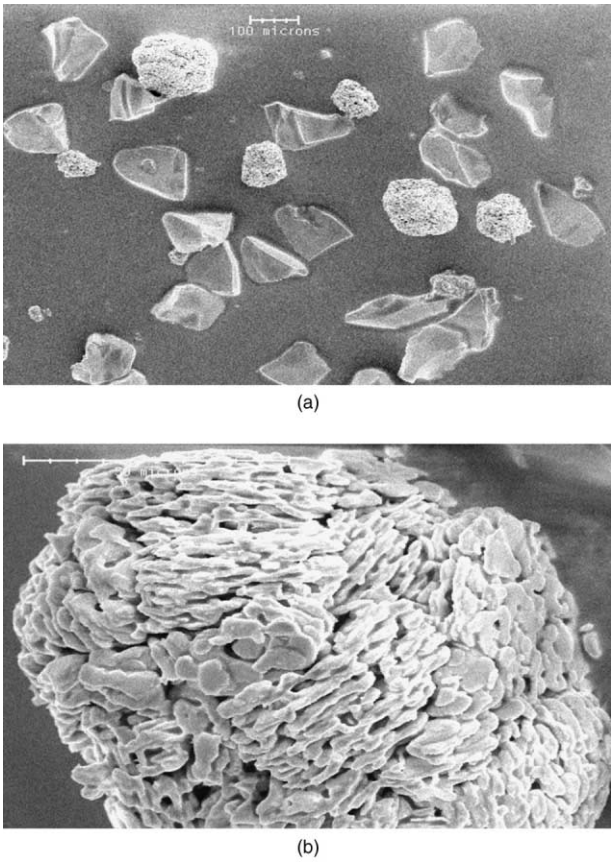

Fig. 8. Scanning electron microscopy images of the SiC–15% Al_2O_3 (wt.%) powders before vaporization experiments: (a) mixture; (b) enlarged view of Al_2O_3 aggregates.

Table 1
Experiment run with the multiple cell device

Cell	Powdered sample	Crucible material	Effusion orifice characteristics	Partial pressures nomenclature
2	SiC (Car.) + 71.8% (weight) Al_2O_3	Graphite (SiC)	h = 2 mm, diam. = 2 mm	p_i (71.8%)
3	SiC (Car.) + 15% (weight) Al_2O_3	Graphite (SiC)	h = 2 mm, diam. = 2 mm	p_i (15%)
4	SiC (Car.) + 5% (weight) Al_2O_3	Graphite (SiC)	h = 2 mm, diam. = 2 mm	p_i (5%)
Gaseous species $i \rightarrow$	Al	Al_2O	CO	SiO
$\frac{p_i\ (5\%)}{p_i\ (71.8\%)}$	1.45±0.12	1.38±0.23	2.09±0.64	0.87±0.1
$\frac{p_i\ (15\%)}{p_i\ (71.8\%)}$	1.44±0.07	1.45±0.12	2±0.53	0.82±0.14
$\frac{p_i\ (5\%)}{p_i\ (15\%)}$	1±0.04	0.95±0.09	1.05±0.11	1.07±0.11

The cells, 2, 3 and 4 are loaded in order to study the influence of the Al_2O_3 composition on the vapor pressures. Graphite cells are coated with SiC (see text). Mean values and standard deviations are for the partial pressures ratios for cells 2, 3 and 4 loaded with different alumina compositions (wt.%). Calculations were performed after discarding the first 5 data (see text).

Table 2
Comparison with the multiple cell device of partial pressures for two cells loaded with the same sample but in two different crucible and lid materials

Cell	Powdered sample	Crucible material	Effusion orifice characteristics	Partial pressures nomenclature
1	SiC (Car.) + 50% (molar) Al_2O_3	Al_2O_3	h = 2 mm, diam = 2 mm	p_i (Al_2O_3)
2	SiC (Car.) + 50% (molar) Al_2O_3	Graphite (SiC)	h = 2 mm, diam = 2 mm	p_i (C)
Gaseous species $i \rightarrow$	Al	Al_2O	CO	SiO
$\frac{p_i\ (Al_2O_3)}{p_i\ (C)}$	0.94 ± 0.02	0.95 ± 0.03	0.73 ± 0.07	1.33 ± 0.1

Mean values and their standard deviations are calculated after discarding the first five data (see text). Graphite cell is coated with SiC (see text).

Table 3
Multiple cell experiment with different loaded samples

Cell	Powder sample	Crucible material	Effusion orifice characteristics	Partial pressures nomenclature
1	25% (molar) SiC (Norton) + 25% Al_2O_3 + 50%C	Graphite SiC	h = 2 mm, diam = 2 mm	p_i (SiC + C) (see Fig. 10)
2	25% (molar) SiC (Norton) + 50% Al_2O_3 + 25%Si	Graphite SiC	h = 2 mm, diam = 2 mm	p_i (SiC + Si) (see Fig. 10)
3	SiC (Norton) + 50% (molar) Al_2O_3	Al_2O_3	h = 2 mm, diam = 2 mm	p_i (Nor.)
4	SiC (Carborundum) + 50% (molar) Al_2O_3	Al_2O_3	h = 2 mm, diam = 2 mm	p_i (Carb.)
Gaseous species $i \rightarrow$	Al	Al_2O	CO	SiO
$\frac{p_i\ (Nor.)}{p_i\ (Carb.)}$	0.55 ± 0.05	0.46 ± 0.06	0.51 ± 0.09	0.69 ± 0.11

Cells 3 and 4 allow the study of the influence of the origin of the SiC powders. Mean values and standard deviations (1450 K < T < 1710 K) of partial pressures ratios are issued from cells 3 and 4. Calculations were performed after discarding the first five data (see text).

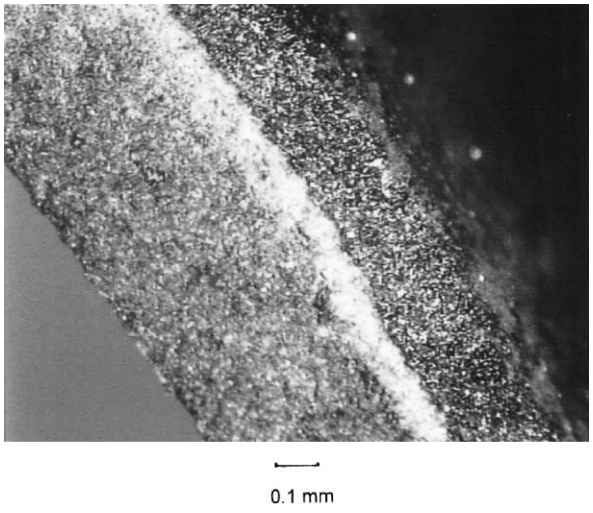

Fig. 9. Optical microscopic observation of the layer formed on the inner walls of a graphite crucible used in the sintering of SiC with Al_2O_3–Y_2O_3 additives.

4.5. SiC–Al_2O_3–Si and SiC–Al_2O_3–C triphasic vaporization

These two triphasic domains could be used as chemical references if their vaporization occurs at equilibrium since the activity of one component can be taken as constant. To check this possibility, we compared the two triphasic partial pressures ratios for each gaseous species to the theoretical ratio calculated from thermodynamics. In Fig. 10, we observe that the experimental ratio is lower for Al, Al_2O and CO and higher for the lone SiO(g) species as compared to equilibrium. After experiment, X-ray analysis of the residues showed that the Al_4C_3 compound had been formed in the SiC–C–Al_2O_3 triphasic sample. We can conclude that at least one of the triphasics is not at equilibrium. These triphasic systems cannot be used as references, and consequently some kinetic limitations occur in their vaporization process as for the pseudobinary SiC–Al_2O_3 (this feature will be analyzed quantitatively in part III).

5. Conclusion

The vaporization of the SiC–Al_2O_3 powders mixtures used as buffer beds in the liquid phase sintering of SiC is analysed in order to further understand mechanisms related both to the loss of matter during sintering and to the enrichment of the SiC compacts with aluminum by the gas phase. The four main species that vaporize are Al(g), Al_2O(g), SiO(g) and CO(g) as predicted by thermodynamics, and their pressures are qualitatively in agreement with the assumption of a congruent vaporization of the SiC–Al_2O_3 pseudobinary system. Consequently, other species such as Si(g) or AlO(g) have very low partial pressures and could not be detected by mass spectrometry: their relative proportions are at least $\leqslant 10^{-4}$.

The impurities included in the basic SiC and Al_2O_3 compounds are quite volatile and are mainly distilled in the temperature increase stage at the beginning of the sintering procedure, and cannot influence the sintering process itself since there are some similarities between our Knudsen cell and the sintering containers: closed

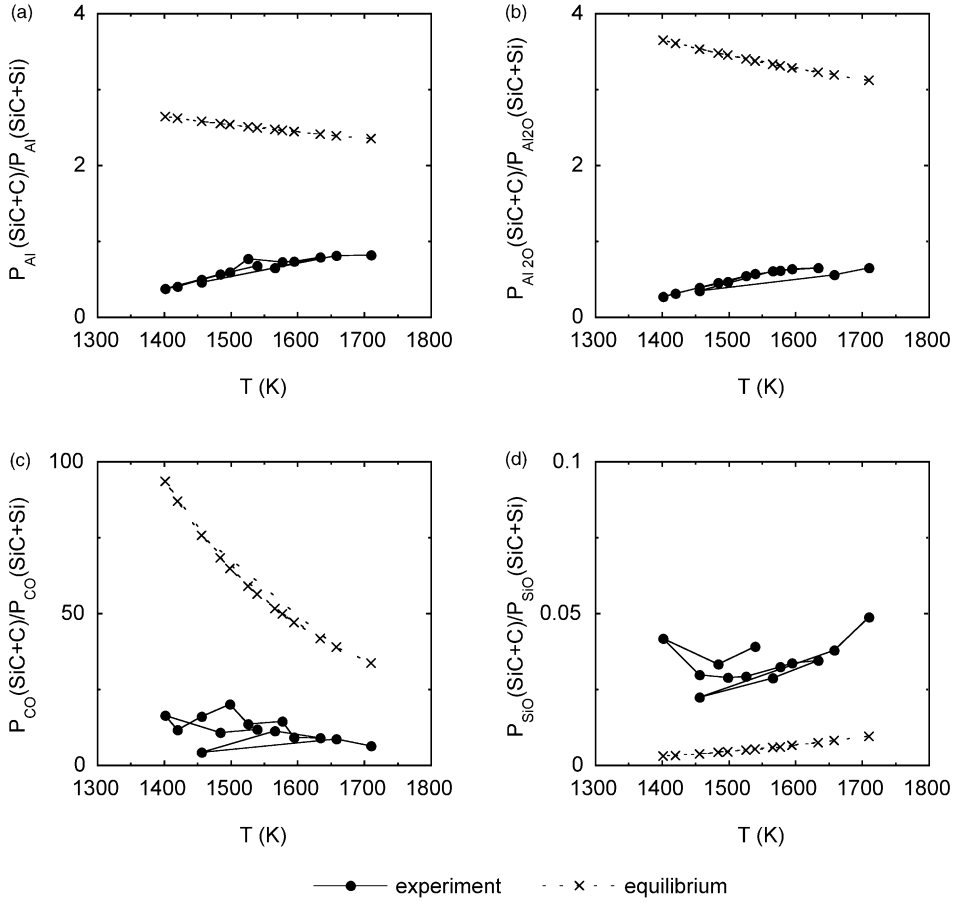

Fig. 10. Partial pressures ratios observed by mass spectrometry (●) or calculated from thermodynamic tables (×) between the two triphasic powder mixtures SiC–Al_2O_3–C and SiC–Al_2O_3–Si: (a) Al(g); (b) Al_2O(g); (c) CO(g); and (d) SiO(g).

vessels, with small orifices, SiC coatings of the walls... that let one assume that matter flow losses ascribed to vaporization flow at the surface of the sample are similar. The same observation works for free Si or C and SiO_2 layers, that are rapidly consumed by vaporization of CO(g) and SiO(g), the pressures of which are already non negligible at rather low temperatures.

The direct comparison of partial pressures with the multiple cell method for different alumina contents, different crucibles (C or alumina), different SiC powders and finally for the two triphasic mixtures SiC–Al_2O_3–Si and SiC–Al_2O_3–C, showed that equilibrium conditions are not reached for these systems. There exists some kinetic barrier to vaporization that can be related to the SiC compound as already observed for mixtures of the ternaries Si–C–O and Si–N–O.[32]

A careful examination of the residues after mass spectrometric experiments or sintering experiments sometimes reveals the precipitation of new compounds like Al_4C_3, or the growth of coating layers of Al_4SiC_4 and SiC on graphite. These phenomena either disturb the congruent vaporization process by concurrent reactions or are the sign of a non congruent behavior due to a kinetic barrier for vaporization. These two possibilities will be analyzed by quantitative evaluation of the evaporation and condensation phenomena in the third part of this series.

References

1. Grande, T., Sommerset, H., Hagen, E., Wiik, K. and Einarsrud, M. A., Effect of weight loss on liquid-phase-sintered silicon carbide. *J. Am. Ceram. Soc.*, 1997, **80**, 1047–1052.
2. Winn, E. J. and Clegg, W. J., Role of the powder bed in the densification of silicon carbide sintered with yttria and alumina additives. *J. Am. Ceram. Soc.*, 1999, **82**, 3466–3470.
3. Nagano, T., Kaneko, K., Zhan, G. D. and Mitomo, M., Effect of atmosphere on weight loss in sintered silicon carbide during heat treatment. *J. Am. Ceram. Soc.*, 2000, **83**, 2781–2787.
4. Baud, S., Frittage en phase liquide du carbure de silicium: évolution des microstructure et des propriétés mécaniques. Etude thermodynamique des interactions oxydes SiC. PhD, Ecole Nationale Supérieure des Mines de Saint Etienne and at Institut National Polytechnique de Grenoble, France, 9 March 2000.
5. Baud, S. and Thevenot, F., Effect of powder bed composition on liquid-phase-sintered silicon carbide, 9th CIMTEC—World Ceramics Congress. In *Ceramics: Getting into the 2000's—Part B*, ed. P. Vincenzini. Techna Srl, Faenza, Italia, 1999, pp. 805–812.
6. Pujar, V. V., Jensen, R. P. and Padture, N. P., Densification of liquid-phase sintered silicon carbide. *J. Mater. Sci. Lett.*, 2000, **19**, 1011–1014.

7. Cordrey, L., Niesz, D. E. and Shanefield, D. J., Sintering of silicon carbide with rare-earth oxide additions. In *Sintering of Advanced Ceramics*, ed. C. A. Handwerker, J. E. Blendell and W. Kaysser. The American Ceramic Society, Inc, Westerville, OH, 1990, pp. 618–636.
8. Gadalla, A., Almasry, M. and Kongkachinchay, P., High temperature reactions within SiC-Al_2O_3 composites. *J. Mater. Res.*, 1992, **7**(9), 2585–2592.
9. Misra, K., Thermochemical analysis of the silicon carbide-alumina reaction with reference to liquid phase sintering of silicon carbide. *J. Am. Ceram. Soc.*, 1991, **74**(2), 345–351.
10. Baud, S., Thevenot, F., Pisch, A. and Chatillon, C., High temperature sintering of SiC with oxide additives. I—Thermodynamic analysis of the vaporization in the SiC-Al_2O_3 and SiC-Al_2O_3-Y_2O_3 systems. *J. Eur. Ceram. Soc.*, in press.
11. Inghram, M. G. and Drowart, J., Mass spectrometry applied to high temperature chemistry. In *High Temperature Technology*. MacGraw Hill, New York, 1959.
12. Drowart, J., Mass spectrometric studies of the vaporization of inorganic substances at high temperatures. In *Condensation and Evaporation of Solids*, ed. E. Rutner, P. Goldfinger and J. P. Hirth. Gordon and Breach, London, 1962, pp. 255–310.
13. Pattoret, A., Drowart, J. and Smoes, S., *Bull. Soc. Fr. Ceram*, 1967, **77**, 75–90.
14. Drowart, J., Pattoret, A. and Smoes, S., *Proc. Br. Ceram. Soc.*, 1967, **8**, 67–89.
15. Chase, M. W., Davies, C. A. and Downey, J. R., et al., JANAF thermochemical tables, 3rd edn. *Journal of Physical and Chemical Reference Data,* 1985, **14**(Suppl. 1).
16. Barin, I., *Thermochemical Data of Pure Substances*. VCH, Weinken D-6940, Germany, 1993.
17. Pankratz, L. B., *Thermodynamic Properties of Elements and Oxides. Bull. 672*. Bureau of Mines, USA, 1982.
18. Pankratz, L. B., Stuve, J. M. and Gokcen, N. A., *Thermodynamic Data for Mineral Technology, Bull. 677*. Bureau of Mines, USA, 1984.
19. Cater, E. D., The effusion method at age 69: current state of the art. In *Characterization of High Temperature Vapors and Gases. N.B.S. Special Publication 561/1*, ed. J. W. Hastie. Nat. Inst. Standards and Technology, Gaitherburg, MD, USA, 1979, pp. 3–38.
20. Dushman, S., *Scientific Foundations of Vacuum Technique*. John Wiley & Sons, New York, 1958 pp. 1–126 (Chapters 1 and 2).
21. Morland, P., Chatillon, C. and Rocabois, P., High-temperature mass spectrometry using the Knudsen effusion cell. I—Optimization of sampling constraints on the molecular beam. *High Temp. Mater. Sci.*, 1997, **37**, 167–187.
22. Chatillon, C., Senillou, C., Allibert, M. and Pattoret, A., High-temperature thermodynamical studies by mass spectrometry: device for measurements using multiple effusion cells. *Rev. Sci. Instrum.*, 1976, **47**(3), 334–340.
23. Chatillon, C., High temperature Knudsen-cell mass spectrometry: III, activity measurements with the multiple cell method. *Electrochem. Soc. Proc.*, 1997, **97**(39), 648–656.
24. Chatillon, C., Malheiros, L. F., Rocabois, P. and Jeymond, M., High temperature mass spectrometry using the Knudsen-cell. II—Technical contraints in the multiple-cell method for activity determinations. *High Temp. High Press.*, 2002, **34**, 213–233.
25. Chatillon, C., Allibert, M. and Pattoret, A., Thermodynamic and physico-chemical behavior of the interactions between Knudsen-effusion-cells and the systems under investigation: analysis by high temperature mass spectrometry. In *Characterization of High Temperature Vapors and Gases*. N.B.S. Special Publication 561/1, ed. J. W. Hastie. Nat. Int. Standards and Technology, Gaitherburg, MD, USA, 1979, pp. 181–210.
26. Chatillon, C., Allibert, M. and Pattoret, A., High temperature thermodynamic studies by mass spectrometry: effect of surface evaporation contribution on the representativity of molecular beam sampling. *High Temp. Sci.*, 1976, **8**, 233–255.
27. Chatillon, C., Evaporation and condensation coefficients by the multiple Knudsen cell mass spectrometric method. In: *Proc. 10th Int. IUPAC Conf. on High Temperature Materials Chemistry*, 10–14 April 2000. Forschungszentrums Jülich Gmbh, Germany, pp. 403–406.
28. Kohl, F. J. and Stearns, C. A., Vaporization of some group IIIA metal—metal oxide systems: mass spectrometric identification of indium gallium oxides (InGaO and $InGaO_2$) and gallium aluminum oxide (GaAlO). NASA Technical Note, TN D-6318, April 1971.
29. Mah, T.-I., Keller, K. A., Sambasivan, S. and Kerans, R. J., High temperature environmental stability of the compounds in the Al_2O_3-Y_2O_3 system. *J. Am. Ceram. Soc.*, 1997, **80**(4), 874–878.
30. Maloney, K. M. and Lynch, D. A., A quantum statistical investigation of the electron impact decompositions of Al_2O, Ga_2O and In_2O. *Int. J. Mass Spectrom. Ion Physics*, 1974, **14**, 415–434.
31. Rocabois, P., Stabilité thermochimique des Composites céramiques base SiC: Approche thermodynamique et expérimentale du Système Si-O-C-N. Thèse INP Grenoble, 1993.
32. Rocabois, P., Chatillon, C. and Bernard, C., High-temperature analysis of the thermal degradation of silicon based materials. II: ternary Si-C-O, Si-N-O and Si-C-N compounds. *High Temp. High Press.*, 1999, **31**, 433–454.
33. Jacobson, N. S., Lee, K. N. and Fox, D. S., Reactions of silicon carbide and silicon(IV) oxide at elevated temperatures. *J. Am. Ceram. Soc.*, 1992, **75**(6), 1603–1611.
34. Rocabois, P., Chatillon, C. and Bernard, C., Thermodynamics of Si-C system II. Mass spectrometric determination of enthalpies of formation of molecules in the gaseous phase. *High Temp. High Press.*, 1995/1996, **27/28**, 25–39.
35. Chatillon, C., Rocabois, P. and Bernard, C., High temperature analysis of the thermal degradation of silicon-based materials: I-binary Si-O, Si-C and Si-N compounds. *High Temp. High Press.*, 1999, **31**, 413–432.